Received: 9 February 2024 | Revised: 19 April 2024 | Accepted: 13 May 2024

DOI: 10.1111/joa.14068

Journal of Anatomy ANATOMICAL SOCIETY WILEY

ORIGINAL ARTICLE

An inclusive anatomical network analysis of human craniocerebral topology

Tim Schuurman[1] | Emiliano Bruner[1,2]

[1]Centro Nacional de Investigación Sobre la Evolución Humana, Burgos, Spain

[2]Alzheimer's Centre Reina Sofía-CIEN Foundation-ISCIII, Madrid, Spain

Correspondence
Tim Schuurman, Centro Nacional de Investigación sobre la Evolución Humana, Paseo Sierra de Atapuerca 3, 09003 Burgos, Spain.
Email: timschrmn@gmail.com

Funding information
Ministerio de Ciencia e Innovación, Grant/Award Number: PID2021-122355NB-C33; Istituto Italiano di Antropologia (ISItA); Fundación Atapuerca/CaixaBank

Abstract

The human brain's complex morphology is spatially constrained by numerous intrinsic and extrinsic physical interactions. Spatial constraints help to identify the source of morphological variability and can be investigated by employing anatomical network analysis. Here, a model of human craniocerebral topology is presented, based on the bony elements of the skull at birth and a previously designed model of the brain. The goal was to investigate the topological components fundamental to the craniocerebral geometric balance, to identify underlying phenotypic patterns of spatial arrangement, and to understand how these patterns might have influenced the evolution of human brain morphology. Analysis of the craniocerebral network model revealed that the combined structure of the body and lesser wings of the sphenoid bone, the parahippocampal gyrus, and the parietal and ethmoid bones are susceptible to sustain and apply major spatial constraints that are likely to limit or channel their morphological evolution. The results also showcase a high level of global integration and efficient diffusion of biomechanical forces across the craniocerebral system, a fundamental aspect of morphological variability in terms of plasticity. Finally, community detection in the craniocerebral system highlights the concurrence of a longitudinal and a vertical modular partition. The former reflects the distinct morphogenetic environments of the three endocranial fossae, while the latter corresponds to those of the basicranium and calvaria.

KEYWORDS
cerebral morphology, functional craniology, integration, modularity, network theory, spatial constraints

1 | INTRODUCTION

The morphology of the human brain and skull reflects, besides function, intrinsic and extrinsic spatial constraints (Bruner et al., 2014; Hofman, 2012; Moss & Young, 1960). Humans have reached a large relative brain size not due to an increase in cortical thickness, but due to a disproportionate expansion in cortical surface (Hofman, 1989, 2014). To accommodate the brain within the limited space of the endocranial cavity, we possess a folded cerebral cortex, probably because of mechanical buckling due to non-uniform surface expansion during development (Ronan & Fletcher, 2015). This is in line with the spatial-packing hypothesis, which suggests that due to the head's finite capacity, once it is spatially optimised, any physical change in one of its components demands subsequent changes in one or more of its neighbouring structures (Jeffery et al., 2021; Jeffery & Manson, 2023; Ross & Ravosa, 1993). Importantly, folding the cerebral cortex implies generating additional intrinsic physical interactions in the brain, which increase its morphological complexity. A notable measure of cortical folding intricacy is the gyrification index, the ratio between the complete and the outer contours of the cortex (Zilles et al., 2013). This parameter presents comparable rostro-caudal patterns of minima and maxima across primates.

The global minimum gyrification index is found in the occipital lobes, while maximal indices are observed in the parieto-temporo-occipital association and frontal cortices (Zilles et al., 1988, 1989). Extrinsically, cerebral spatial arrangement is affected by interplay with the enveloping skull, according to the cranial functional matrix hypothesis (Bruner et al., 2014; Moss & Young, 1960; Richtsmeier & Flaherty, 2013).

Craniocerebral spatial constraints are particularly meaningful for palaeoneurology. In this field of research, endocranial casts of extinct species are used as proxies to make inferences regarding brain evolution (Bruner, 2017, 2019; Dumoncel et al., 2021; Holloway et al., 2004). This is a demanding task, since it is often challenging to tell apart primary changes caused by functional adaptation (cognition and behaviour) from secondary changes due to spatial constraints and topological rearrangements (Bruner, 2015, 2019). To deal with this issue, topology has been employed to research the morphological attributes of anatomical systems through the application of network analysis (Dos Santos et al., 2017; Esteve-Altava et al., 2011; Kerkman et al., 2018; Murphy et al., 2018). In network theory, topology refers to the structural or functional relation among the components of a system (Rashevski, 1954). Under this lens, morphological organisation stems from the interactions between anatomical elements (Rasskin-Gutman & Buscalioni, 2001). Anatomical network analysis hence evaluates the topology of an anatomical system based on the principle of physical contact among its components to investigate spatial constraints. Within this framework, this approach is intended as an exploratory tool to investigate the components that are fundamental to the craniocerebral geometric balance, and to identify underlying phenotypic patterns of spatial arrangement. Beyond modelling, specific hypotheses should be tested on experimental grounds, or using developmental series able to reveal the dynamic aspects of the underlying morphogenetic system.

Several studies have used anatomical network analysis to investigate the evolution of the morphology of the human brain and skull separately (Bruner, 2022; Esteve-Altava et al., 2011; Esteve-Altava, Marugán-Lobón, Botella, Bastir, & Rasskin-Gutman, 2013; Schuurman & Bruner, 2023, 2024), and only one has presented an anatomical network model that combines both (Bruner et al., 2019). Anatomical network analysis of the skull revealed the notable structural relevance of the ethmoid and sphenoid bones, as well as their vital roles as a local hub and a connector hub of the network, respectively (Esteve-Altava, Marugán-Lobón, Botella, Bastir, & Rasskin-Gutman, 2013). In other words, the ethmoid bone is crucial to promote integration among its nearest neighbours, while the sphenoid bone has a major role in integrating different parts of the network. The contribution of the sphenoid bone to the derived organisation of the modern human skull is debated (Lieberman, 1998; Spoor et al., 1999). Nevertheless, a comparative analysis of *Macaca nemestrina* and modern humans suggests that ontogenetic differences in the sphenoid bone's synchondroses influence cranial base angulation, a major determinant in the adult phenotype of the skull (Jeffery, 1999). From a global standpoint, using community detection algorithms, the anatomical network model of the skull can be divided longitudinally into two morphological modules: an anterior facial block, or viscerocranium, and a posterior cranial block, or neurocranium (Esteve-Altava, Marugán-Lobón, Botella, Bastir, & Rasskin-Gutman, 2013). Conversely, network approaches to the brain, first using Brodmann's map and then a traditional macro-anatomical division, stressed the structural relevance of the limbic lobes (Bruner, 2022; Schuurman & Bruner, 2023). The deep medial counterpart to the temporal lobes, the parahippocampal gyrus, was found to be especially significant (Schuurman & Bruner, 2023). A comprehensive overview of modularity and community detection in human brain morphology then found the simultaneous presence of a longitudinal and a vertical modular partition of the brain's topology (Schuurman & Bruner, 2024). This combination of patterns corresponds with the organisation of the enveloping braincase: its longitudinal division based on topology is in line with the different morphogenetic environments of the three endocranial fossae (Bruner & Ripani, 2008; Esteve-Altava, Marugán-Lobón, Botella, Bastir, & Rasskin-Gutman, 2013; Jeffery & Spoor, 2004; Lieberman et al., 2000a), while its vertical gradient matches the distinct ontogenetic processes associated with the basicranium (lower neurocranium) and calvaria (upper neurocranium) (Bastir et al., 2006; Lieberman et al., 2000a; Sperber & Sperber, 2018). Lastly, an early evaluation of the relationship between brain and braincase considered only a few neurocranial elements and did not include any subcortical brain regions (Bruner, 2019). Its results showcased the lateral temporal cortex as highly burdened due to its longitudinal span, and evidenced a longitudinal modular partition of the brain comprising an independent prefrontal cortex and a highly integrated posterior block separated by the precentral gyrus (Bruner et al., 2019).

Here, we incorporate all the previous information into a single, cohesive assessment of human craniocerebral topology, by merging previous detailed anatomical network models of the brain and skull and hence increasing the resolution of an early combined approach (Bruner, 2022; Bruner et al., 2019; Esteve-Altava et al., 2011; Esteve-Altava, Marugán-Lobón, Botella, Bastir, & Rasskin-Gutman, 2013; Schuurman & Bruner, 2023, 2024). Our aim is to identify regions fundamental in the geometric balance of the brain and skull, as to detect overarching phenotypic patterns of spatial arrangement, for a wider, integral view of brain morphology in ontogeny and phylogeny.

2 | MATERIALS AND METHODS

2.1 | The human craniocerebral anatomical network model

An anatomical network model of the adult skull was built according to its bony elements at birth (Sperber & Sperber, 2018; White et al., 2013). In humans, the most crucial steps in the topological organisation of the head occur in the first 2 years after birth, when the spatial constraints of the uterus are lifted (Leigh, 2004; Lieberman & McCarthy, 1999; Neubauer et al., 2009; Neubauer & Hublin, 2012;

Wilder & Semendeferi, 2022). Hence, a model based on the cranial elements at birth allows to investigate most extensively the spatial constraints of the head during morphogenesis. The nodes of the model formalise the skull's bony elements, whether ossification centres, bone parts or complete bones. Meanwhile, the edges represent the skull's joints, whether synchondroses or sutures. This model was then added to a previously designed anatomical network model of the brain, based on traditional macroanatomical divisions, which spans the entire telencephalon, diencephalon and rhombencephalon (Schuurman & Bruner, 2023). The final craniocerebral network incorporates 76 distinct components, for a total of 133 nodes and 552 edges if paired elements are counted separately (Figure 1). The network and corresponding variables were modelled, analysed and visualised using Gephi 0.10.1, PAST 4.0 and R (Bastian et al., 2009; Hammer et al., 2001; R Core Team, 2023). For R, the specific functions that we employed were part of the package 'igraph' (Csardi & Nepusz, 2006).

Two noteworthy considerations were made regarding the cranial components. The first one is in relation to the mandible. Since the mandible is an isolated, not sutured bone, it was excluded from the model (Esteve-Altava et al., 2011). A second issue concerns two small structures tightly related to the temporal bone: the styloid process (tympanohyal part and stylohyal part) and the ear ossicles (malleus, incus and stapes). The styloid process fuses with the temporal bone during early infancy, while the ear ossicles develop embedded partly within it. Hence, instead of considering these elements as separate nodes in the network, we included them within the temporal bone's petromastoid block ('petromastoid' from here on) to emphasise the main skull bones (Esteve-Altava et al., 2017).

2.2 | Statistical analysis

Anatomical network analysis considers, at the same time, the level of the individual anatomical elements, and the level of the anatomical system in its entirety. In this study, we employ a set of standard metrics commonly used in network analysis, which are presented and explained in much detail elsewhere (e.g. Newman, 2018; Rasskin-Gutman & Esteve-Altava, 2014). At the level of the individual craniocerebral components, five normalised centrality metrics were measured that inform about the topological relevance, and consequently morphological complexity, of the nodes (Newman, 2018; Rasskin-Gutman & Esteve-Altava, 2014). *Degree* concerns a node's significance as a hub of the system. *Closeness* denotes the spatial proximity of a node to the others within the network. *Betweenness* refers to a node's bridging capability among the major regions of the network. *Eigenvector centrality* informs about a node's significance according to the degree of its neighbours. Lastly, *clustering coefficient* quantifies a region's inherent level of integration by measuring the relative number of interactions among a node's neighbours. Notably, the probability that all neighbours of a single node interact is inversely proportional to its number of edges (degree). The centrality metrics also contribute to identifying the part that each node plays in the network, and

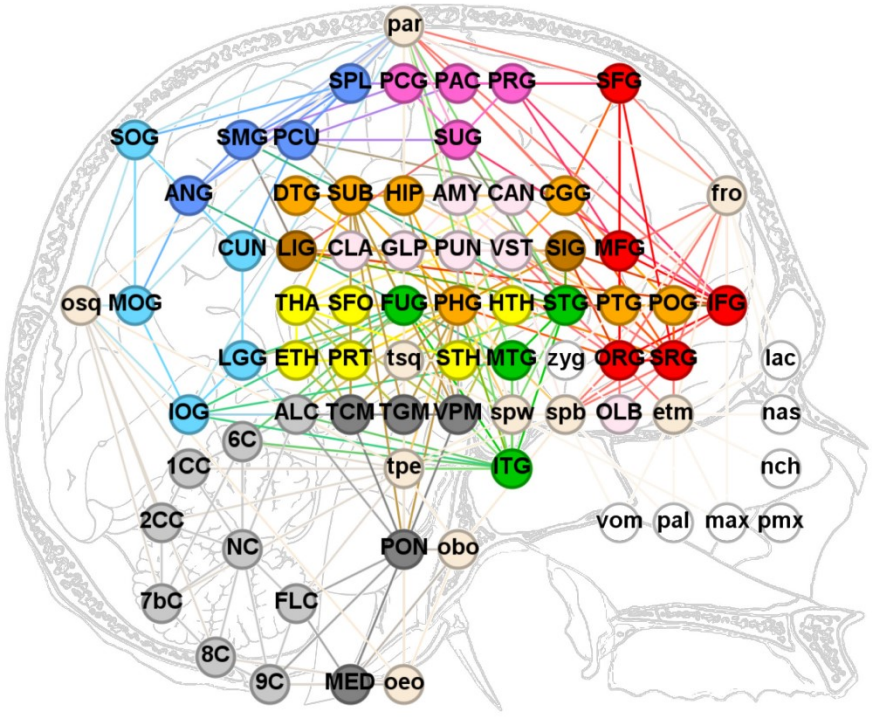

FIGURE 1 Anatomical layout of the craniocerebral network employed in this study showing a medial view of the left side of the head and the elements used in this model. Colours: neurocranium: bone white; viscerocranium: white; frontal lobe: red; central lobe: dark pink; parietal lobe: dark blue; temporal lobe: green; occipital lobe: light blue; insular lobe: brown; limbic lobe: orange; basal and subcortical telencephalon: light pink; diencephalon: yellow; cerebellum: light grey; brainstem: dark grey. See Table 1 for labels.

thus their addition to the geometric balance of the system. The relation between degree and betweenness is especially remarkable. Degree informs about a node's participation in the local integration of the anatomical system in question. On the other hand, betweenness stresses a node's contribution to the anatomical system's global integration (Bruner et al., 2019; Rasskin-Gutman & Esteve-Altava, 2014).

In regard to the craniocerebral complex as a whole, four variables were observed which assess its morphological complexity and architecture (Esteve-Altava, Marugán-Lobón, Botella, & Rasskin-Gutman, 2013; Newman, 2018; Rasskin-Gutman & Esteve-Altava, 2014; Schuurman & Bruner, 2023). *Network density* reflects the completeness of the network. *Mean clustering coefficient* measures the global integration of the network. *Average path length* assesses the network's communication efficiency. Presently, since we are dealing with physical interactions among anatomical elements, this parameter evaluates the system's efficiency in the diffusion of biomechanical or morphogenetic forces. *Degree distribution* measures heterogeneity, that is, the variance in the number of interactions among a network's nodes. Subsequently, heterogeneity signals a pattern of specialised anatomical elements with distinct structural functions, a phenomenon called anisomerism. Additionally, four properties were tested of morphological organisation of the brain and skull, and their topological dynamics (Blondel et al., 2008; Newman, 2018; Rasskin-Gutman & Esteve-Altava, 2014; Schuurman & Bruner, 2024; Wuchty et al., 2006). The *small-world effect* indicates an intermediate state of order in the network's edges. A *scale-free topology* is observed when the network's degree distribution resembles that of a power-law, differentiating it from random networks. Craniocerebral *modularity* was evaluated using the Louvain method for community detection. Due to an element of stochasticity in the algorithm, it was run 10,000 times for optimisation of Newman and Girvan's (2004) modularity function Q, a quantitative criterion for the quality of network partitions. Finally, *hierarchy* combines a scale-free topology with a modular structure. In hierarchical networks, modules are composed of smaller sub-modules, formed by nodes with low degree and integrated by nodes with high degree.

3 | RESULTS

3.1 | Local analysis

Values of local variables for all nodes in the network are presented in Table 1. The parahippocampal gyrus or the combined structure of the body and lesser wings of the sphenoid bone ('sphenoid body and lesser wings' from here on) exhibit both high degree and betweenness, meaning they contribute to the local and global integration of the craniocerebral system; they act as connector hubs. The ethmoid bone presents a high degree and low betweenness, and hence represents a local hub: its importance lies mostly in its contribution to the local integration of its neighbouring craniocerebral components. The cingulate gyrus, with its low degree and high betweenness, participates primarily in the system's global integration, by bridging the frontal, central, parietal and limbic lobes, as well as the two hemispheres. Finally, the nasal concha or the claustrum, which possess a very low degree and betweenness, act as satellite anatomical elements because their topological addition to the craniocerebral system is almost null.

Degree, closeness, betweenness and eigenvector share a significant positive correlation ($r = 0.87 \pm 0.07$, $p < 0.001$). On the other hand, clustering coefficient shares a significant negative correlation with all other metrics ($r = -0.48 \pm 0.06$, $p < 0.001$) (Table 2). A more detailed analysis using regression models of the correlations among the centrality metrics yields valuable insight on specific nodes (Figure 2): in particular, the high betweenness (how much a node is interposed among the other ones) of the parahippocampal gyrus is due especially to its high degree (number of interactions), while the high betweenness of the sphenoid body and lesser wings is more associated with its high closeness (spatial proximity within the network).

A principal component analysis (PCA) based on the correlation matrix of all five centrality metrics yields a first component that explains a 79% of the variance (PC1) (Figure 3a) and a second component that explains 14% of the variance (PC2). PC1 is associated with an increase in degree, closeness, betweenness and eigenvector (Figure 3c), and can thus be interpreted as a vector of general increase in topological complexity. The elements scoring highest on PC1 are the sphenoid body and lesser wings, the parahippocampal gyrus, parietal bone and ethmoid bone. The lowest scoring elements are the claustrum, subfornical organ, subthalamus and olfactory bulb (Figure 4). PC2 explains an amount of variance inferior to the original variables independently ($\lambda < 1$) (Figure 3b), and will therefore not be considered further.

3.2 | Global analysis

Concerning the global variables, the craniocerebral network shows a density of 0.06, an average path length of 2.97 and a mean clustering coefficient of 0.48. That is to say, the 552 edges of the network represent merely a 6% of all possible interactions; a pair of nodes is separated, on average, by two other elements; and almost half of the nodes' neighbours are interconnected. As for its architecture, the network's degree distribution is heavily right-skewed, signalling a high variance in the nodes' degree. Nevertheless, instead of fitting a power-law function, the degree distribution is patently Gaussian (Figure 5). Consequently, we cannot affirm that the topology of the craniocerebral anatomical network model is scale-free or hierarchical.

Since, compared with a sample of 10,000 equivalent random Erdös-Rényi networks (Erdös & Rényi, 1960), the mean clustering coefficient of the craniocerebral network is much larger ($C_{random} = 0.06$; $C_{brain} = 0.48$) and its average path length is similar ($L_{random} = 2.53$; $L_{brain} = 2.97$), the index of small-worldness satisfies

TABLE 1 Brain and skull nodes, centrality metrics, and principal component 1 (PC1) scores.

	Label	Degree	Closeness	Betweenness	Eigenvector	Clustering	PC1
Neurocranium							
Frontal bone, half	fro	0.11	0.41	0.05	0.56	0.31	2.80
Parietal bone	par	**0.16**	0.40	**0.11**	0.66	0.23	**4.97**
Temporal bone, squama	tsq	0.05	0.34	0.00	0.30	0.67	−0.70
Temporal bone, petromastoid	tpe	0.12	**0.43**	**0.06**	**0.71**	0.25	**3.85**
Occipital bone, squama	osq	**0.13**	0.39	**0.06**	0.53	0.21	3.15
Occipital bone, exoccipital	oeo	0.05	0.35	0.01	0.25	0.43	−0.31
Occipital bone, basioccipital	obo	0.05	0.37	0.01	0.33	0.43	0.23
Ethmoid bone	etm	**0.16**	0.40	**0.08**	0.63	0.23	**4.32**
Sphenoid bone, body and lesser wings	spb	**0.15**	**0.47**	**0.14**	**0.96**	0.21	**7.01**
Sphenoid bone, pterygoids and greater wings	spw	0.10	**0.42**	0.04	0.60	0.37	2.73
Viscerocranium							
Premaxilla, ossification centre	pmx	0.02	0.26	0.00	0.03	0.00	−1.91
Maxilla, ossification centre	max	0.08	0.34	0.03	0.30	0.27	0.77
Palatine, bone	pal	0.05	0.34	0.00	0.23	0.60	−0.89
Vomer, ossification centre	vom	0.04	0.34	0.00	0.21	0.70	−1.21
Nasal concha, bone	nch	0.03	0.30	0.00	0.12	**0.83**	−2.23
Lacrimal, bone	lac	0.03	0.31	0.00	0.15	**0.83**	−2.01
Nasal, bone	nas	0.03	0.31	0.00	0.15	0.67	−1.76
Zygomatic, bone	zyg	0.03	0.32	0.00	0.16	0.67	−1.63
Frontal lobe							
Superior frontal gyrus	SFG	0.07	0.37	0.02	0.31	0.33	0.67
Middle frontal gyrus	MFG	0.05	0.35	0.00	0.24	0.73	−0.93
Inferior frontal gyrus	IFG	0.08	0.35	0.01	0.36	0.42	0.39
Straight gyrus	SRG	0.10	0.39	0.04	0.49	0.29	2.20
Orbital gyrus	ORG	0.09	0.40	0.03	0.54	0.35	2.12
Central lobe							
Precentral gyrus	PRG	0.05	0.31	0.00	0.20	0.52	−1.04
Postcentral gyrus	PCG	0.05	0.30	0.00	0.15	0.53	−1.42
Paracentral lobule	PAC	0.05	0.31	0.01	0.11	0.27	−0.98
Subcentral gyrus	SUG	0.05	0.31	0.00	0.20	0.62	−1.14
Parietal lobe							
Superior parietal lobule	SPL	0.05	0.32	0.00	0.14	0.40	−1.01
Precuneus	PCU	0.05	0.35	0.02	0.16	0.13	0.03
Supramarginal gyrus	SMG	0.05	0.31	0.00	0.18	0.52	−1.04
Angular gyrus	ANG	0.04	0.30	0.00	0.14	0.50	−1.60
Temporal lobe							
Superior temporal gyrus	STG	0.08	0.34	0.01	0.33	0.47	0.13
Middle temporal gyrus	MTG	0.05	0.33	0.00	0.27	0.62	−0.79
Inferior temporal gyrus	ITG	0.08	0.39	0.01	0.53	0.51	1.31
Fusiform gyrus	FUG	0.07	0.37	0.01	0.46	0.50	0.55
Occipital lobe							
Superior occipital gyrus	SOG	0.04	0.31	0.01	0.15	0.40	−1.15
Middle occipital gyrus	MOG	0.04	0.31	0.00	0.17	0.60	−1.43

TABLE 1 (Continued)

	Label	Degree	Closeness	Betweenness	Eigenvector	Clustering	PC1
Inferior occipital gyrus	IOG	0.06	0.35	0.01	0.33	0.39	0.14
Cuneus	CUN	0.03	0.29	0.00	0.06	0.00	−1.21
Lingual gyrus	LGG	0.05	0.35	0.01	0.26	0.40	−0.34
Insular lobe							
Short insular gyri	SIG	0.05	0.35	0.01	0.27	0.48	−0.26
Long insular gyri	LIG	0.06	0.32	0.01	0.22	0.39	−0.40
Limbic lobe							
Cingulate gyrus	CGG	0.05	0.37	0.02	0.22	0.24	0.26
Parahippocampal gyrus	PHG	**0.17**	**0.45**	**0.13**	**1.00**	0.21	**6.98**
Paraolfactory gyrus	POG	0.03	0.30	0.00	0.10	0.33	−1.48
Paraterminal gyrus	PTG	0.05	0.32	0.01	0.21	0.43	−0.76
Hippocampus proper	HIP	0.06	0.34	0.00	0.37	0.54	−0.28
Dentate gyrus	DTG	0.03	0.32	0.00	0.19	**0.83**	−1.83
Subiculum	SUB	0.08	0.35	0.01	0.48	0.47	0.54
Basal and subcortical telencephalon							
Olfactory bulb	OLB	0.02	0.32	0.00	0.15	**1.00**	−2.24
Amygdaloid complex	AMY	0.06	0.33	0.00	0.30	0.54	−0.50
Globus pallidus	GLP	0.05	0.30	0.00	0.22	0.73	−1.61
Caudate nucleus	CAN	0.08	0.33	0.00	0.35	0.47	−0.02
Putamen nucleus	PUN	0.09	0.36	0.03	0.44	0.33	1.38
Ventral striatum	VST	0.09	0.38	0.02	0.49	0.39	1.60
Claustrum	CLA	0.02	0.28	0.00	0.09	**1.00**	−2.86
Diencephalon							
Thalamus	THA	0.11	0.35	0.02	0.54	0.33	1.64
Epithalamus	ETH	0.03	0.29	0.00	0.15	**0.83**	−2.24
Hypothalamus	HTH	0.07	0.34	0.01	0.31	0.36	0.14
Subthalamus	STH	0.02	0.28	0.00	0.12	0.67	−2.29
Pretectum	PRT	0.06	0.37	0.01	0.41	0.61	0.21
Subfornical organ	SFO	0.02	0.28	0.00	0.10	**1.00**	−2.87
Cerebellum							
Anterior lobe	ALC	0.12	**0.42**	0.05	**0.76**	0.29	3.60
VI	6C	0.08	0.36	0.01	0.46	0.38	0.84
Crus I	1CC	0.05	0.33	0.00	0.22	0.67	−1.14
Crus II	2CC	0.05	0.34	0.00	0.27	0.62	−0.68
VIIb	7bC	0.05	0.34	0.00	0.28	0.52	−0.49
VIII	8C	0.05	0.30	0.00	0.17	0.47	−1.35
IX	9C	0.05	0.30	0.00	0.18	0.52	−1.19
Flocculonodular lobe	FLC	0.05	0.35	0.00	0.24	0.27	−0.28
Nuclei	NC	0.07	0.31	0.00	0.26	0.31	−0.39
Brainstem							
Midbrain tectum	TCM	0.09	0.38	0.02	0.60	0.47	1.71
Midbrain tegmentum	TGM	0.09	0.38	0.01	0.63	0.55	1.37
Midbrain ventral portion	VPM	0.11	0.39	0.03	**0.67**	0.34	2.64
Pons	PON	0.11	0.39	0.04	0.63	0.32	2.49
Medulla oblongata	MED	0.05	0.31	0.00	0.17	0.67	−1.47

Numbers in bold indicate the five highest values for each variable.

TABLE 2 Pearson's correlation among the centrality metrics.

R/p-value	Degree	Closeness	Betweenness	Eigenvector	Clustering
Degree		**5.67E−25**	**5.56E−25**	**1.98E−35**	**3.65E−07**
Closeness	0.87		**1.06E−17**	**1.11E−33**	**2.34E−05**
Betweenness	0.87	0.79		**1.19E−19**	**6.00E−06**
Eigenvector	0.94	0.93	0.82		**1.62E−04**
Clustering	−0.54	−0.46	−0.49	−0.42	

Numbers in bold indicate p-values < 0.05.

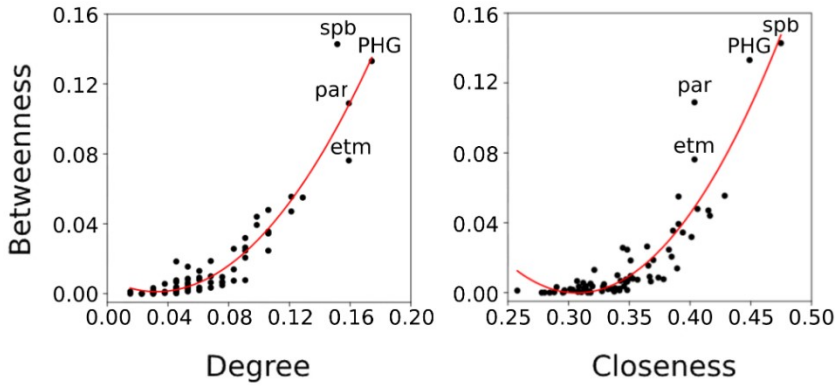

FIGURE 2 Regression models of the relations between degree and betweenness, and closeness and betweenness. Labels: etm: ethmoid bone; par: parietal bone; PHG: parahippocampal gyrus; spb: sphenoid bone, body and lesser wings.

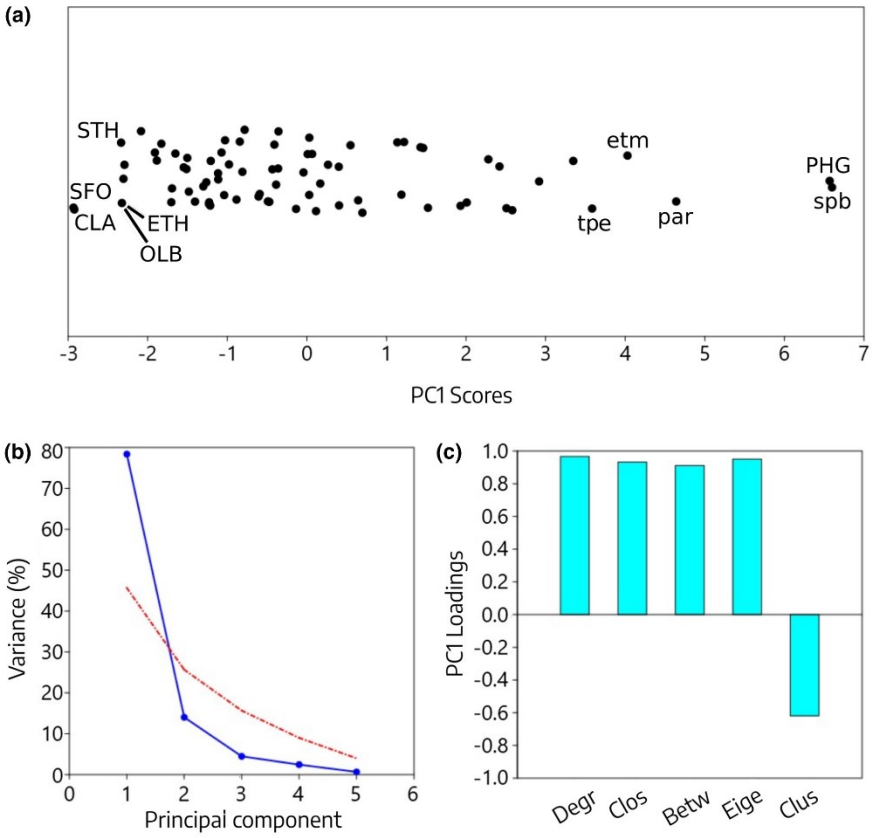

FIGURE 3 Jitter plot of the principal component 1 (PC1) scores for each node of the anatomical network model of the human brain and skull (a). According to the scree plot, only PC1 is significant (b), and it is associated with an increase in all centrality metrics except clustering coefficient (c). Labels: CLA, claustrum; etm, ethmoid bone; ETH, epithalamus; OLB, olfactory bulb; par, parietal bone; PHG, parahippocampal gyrus; SFO, subfornical organ; spb, sphenoid bone, body and lesser wings; STH, subthalamus; tpe, temporal bone, petromastoid.

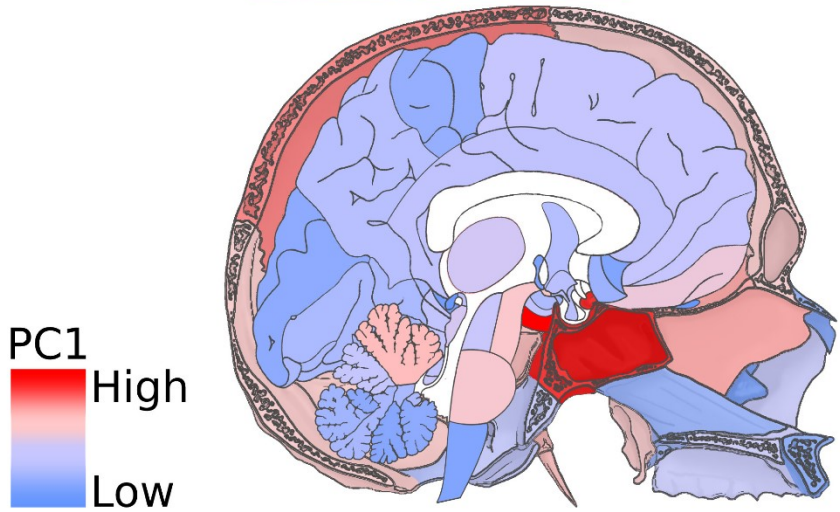

FIGURE 4 Principal component 1 (PC1) scores, represented through a chromatic scale on an anatomical illustration of a medial view of the left side of the human brain and skull.

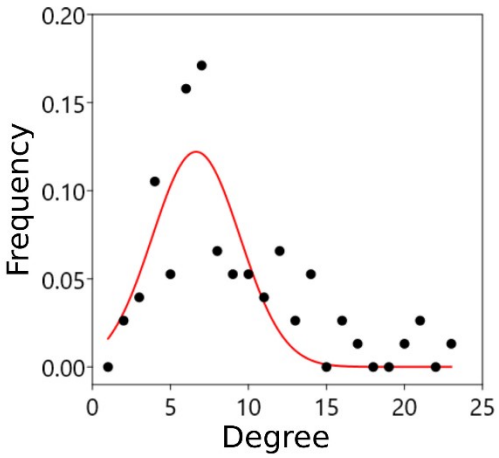

FIGURE 5 Regression model of the degree distribution.

S^{WS} >0.012*n*, where '*n*' is the number of nodes of the network (S^{WS}=6.47) (Humphries & Gurney, 2008; Rasskin-Gutman & Esteve-Altava, 2014). Hence, the craniocerebral anatomical network model does display the small-world effect.

Analysis of the network's modularity yields six modules, with a quality value of Q=0.56±0.02 (Figure 6). In relation to the brain, the Louvain method for community detection finds, first, a single posterior inferior module, incorporating the cerebellum, pons and medulla oblongata. Second, a left and a right anterior inferior module, which span the inferior aspects of the frontal lobes, the limbic lobes (except the right cingulate gyrus), the left insula, and the basal and subcortical telencephalon (except the claustrum), as well as the entire diencephalon and midbrain. And third, a left and a right superior module that consist of the superior aspects of the frontal lobes, as well as the entire central, parietal, temporal and occipital lobes. Only the left and right anterior inferior modules are exclusively cerebral. Regarding the skull, all bony components that are not in contact with the brain (i.e. the viscerocranium), together with the left and right halves of the frontal bone, the ethmoid bone and the sphenoid body and lesser wings, form an exclusively cranial anterior module. The rest of the skull, most of the neurocranium, is divided vertically. Inferior elements, including the petromastoid or the entire occipital bone, are included with the brain in the posterior inferior module. Meanwhile, superior elements, the combined structure of the pterygoids and greater wings of the sphenoid bone, the parietal bone, and the temporal squama, are incorporated with the brain in the left and right superior modules. Due to the stochastic nature of the computational steps of the Louvain method for community detection, asymmetries are found in the modules to which paired elements are assigned. Instances of asymmetry in the different communities include the cingulate gyrus, insula, and claustrum. In all three cases, the left representatives of each pair of elements belong to the left superior module, while their right counterparts pertain to the right anterior inferior module.

4 | DISCUSSION

Multiple preliminary studies have employed anatomical network analysis to identify spatial constraints that affect the morphology and morphogenesis of the brain and skull separately, as well as jointly (Bruner, 2022; Bruner et al., 2019; Esteve-Altava et al., 2011; Esteve-Altava, Marugán-Lobón, Botella, Bastir, & Rasskin-Gutman, 2013; Schuurman & Bruner, 2023, 2024). However, when compared with previous network analyses of the human skull (Esteve-Altava et al., 2011, 2017; Esteve-Altava, Marugán-Lobón, Botella, Bastir, & Rasskin-Gutman, 2013), this approach yields a more exhaustive model of the cranial anatomical system. Here, we aim to provide a comprehensive topological understanding of the human craniocerebral spatial arrangement. This is achieved by combining previous detailed anatomical network models of the brain and skull, thereby increasing the resolution of an early combined approach.

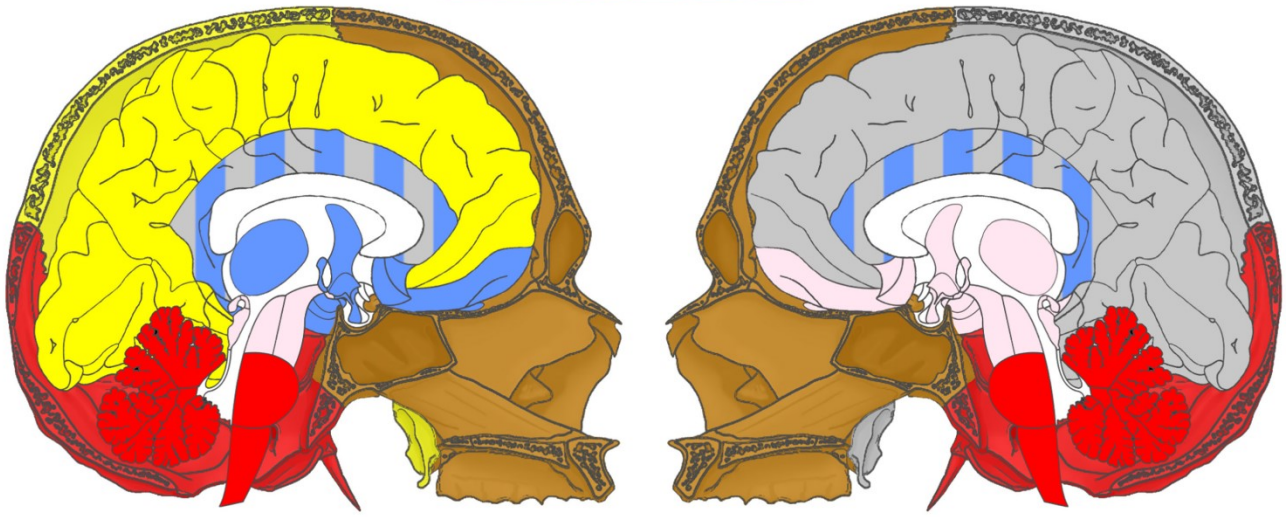

FIGURE 6 Topological modules, represented on an anatomical illustration of a medial view of the left and right sides of the human brain and skull. Striped patterns identify community assignment to distinct modules.

4.1 | Morphological interpretation of the local variables

Physical interactions among craniocerebral components create co-dependencies that translate into spatial constraints (Esteve-Altava, Marugán-Lobón, Botella, Bastir, & Rasskin-Gutman, 2013; Rasskin-Gutman & Esteve-Altava, 2018). This phenomenon brings about the concept of *burden*: the magnitude of spatial constraint to which an anatomical element is subjected (Riedl, 1978). The concept of burden has two implications: one is that the probability of primary change in a craniocerebral component (change due to functional adaptation) is bound by the weight of its co-dependencies; the other is that sets of highly burdened elements are likely to belong to a common body plan. In other words, highly burdened elements are more liable to secondary change (alterations enforced by modifications in nearby elements), while simultaneously possessing a higher capacity to produce secondary changes themselves (Bruner et al., 2019). Therefore, if a morphological alteration is observed in a craniocerebral component, declaring functional adaptation as the source should be done only after rejecting any secondary influences.

Using a PCA based on the five centrality metrics we found that the sphenoid body and lesser wings, the parahippocampal gyrus, parietal bone, and ethmoid bone present a high morphological complexity, which makes them prone to simultaneously sustain and enforce a large amount of spatial constraints. Brain and skull comprise a morphogenetic system in equilibrium, with parallel architectural trajectories in ontogeny and phylogeny. Concerning the aforementioned craniocerebral components, this leads spatial constraints to limit and channel the morphological evolution of their own, as well as other anatomical elements (Bastir, 2008; Bastir et al., 2010; Cheverud, 1996; Moss & Young, 1960; Richtsmeier et al., 2006; Richtsmeier & Flaherty, 2013). The burden of the sphenoid body and lesser wings is likely due to its central position within the network. The parahippocampal gyrus owes most of its burden to the highly interregional character of its interactions: it is a bridge between elements as distant as the orbital and lingual gyri, and as an interface between soft and hard tissues of the head. Lastly, the burden of the parietal and ethmoid bones is due to their large number of interactions.

Nonetheless, there is a noteworthy difference between the parietal bone and the rest of these elements. The parietal bone interacts with multiple brain elements associated with distinct morphogenetic regions. Because of its peripheral position, it shows no severe spatial conflicts with other cranial elements (although it is constrained between the frontal and the occipital squamae) (Bruner, 2004). As a result, in both ontogeny and phylogeny, the parietal bone is passively moulded by the different factors involved in brain variation (Bruner et al., 2015, 2019; Moss & Young, 1960). In the case of the sphenoid body and lesser wings, parahippocampal gyrus and ethmoid bone the opposite condition seems to be the case: the skull moulds the brain (Bastir et al., 2008; Jeffery & Manson, 2023; Lieberman, 1998; Lieberman et al., 2000a; Moss & Young, 1960). Regarding the temporal lobes, including their deep medial counterpart (the parahippocampal gyrus), there is a disagreement on whether they show morphological changes in modern humans (Pearson et al., 2023; Rilling, 2023; Rilling & Seligman, 2002). Considering their spatial position and burden, we can nevertheless suppose that their gross morphology is probably affected by secondary influences: spatial constraints unrelated with the evolution of the brain (Bruner, 2022; Bruner et al., 2019; Schuurman & Bruner, 2023).

4.2 | Morphological interpretation of the global variables

The complex spatial accommodation of the craniocerebral complex, and the head as a whole, is regulated by different levels of modularity and integration (Bastir et al., 2006; Lieberman, 2011). The basic

modules of the head, including the brain, are semi-independent from each other. In this context, the skull is particularly relevant, as it mediates the physical interactions among the various other encephalic structures (e.g. Toro-Ibacache et al., 2016). Nonetheless, all anatomical elements, including the brain, exert tensions and pressures that mould and constrain the surrounding components, contributing to the morphogenesis of the adult phenotype and generating an integrated anatomical system (Bastir et al., 2004; Bastir & Rosas, 2005; Bruner, 2015; Enlow et al., 1971; Lieberman, 2011). Regarding craniocerebral integration, brain and skull conform a morphogenetic complex in equilibrium, which leads the different modules to change in ways that can accommodate each other properly throughout ontogeny and phylogeny (Bastir, 2008; Bastir et al., 2010; Cheverud, 1996; Lieberman, 2011; Moss & Young, 1960; Richtsmeier et al., 2006; Richtsmeier & Flaherty, 2013).

The craniocerebral network's degree distribution signals anisomerism. Anisomerism measures an anatomical system's morphological complexity in terms of the structural specialisation of its elements, resulting in increased levels of global integration (higher mean clustering coefficient) and diffusion of biomechanical forces through physical interaction (shorter average path length). These factors are essential to channel morphological variation and, overall, an evolutionary advantage in regard to plasticity (Esteve-Altava, Marugán-Lobón, Botella, & Rasskin-Gutman, 2013). Furthermore, high levels of global integration and efficient diffusion of biomechanical forces lead the craniocerebral network, as many other biological systems, to exhibit the small-world effect (Esteve-Altava, Marugán-Lobón, Botella, Bastir, & Rasskin-Gutman, 2013; Rasskin-Gutman & Esteve-Altava, 2014). This is especially relevant in the case of the brain, since its morphology shares common factors and reciprocal influences with neural connectivity, as observed for instance in the cingulate gyrus and precuneus (Bullmore & Sporns, 2009, 2012; Hagmann et al., 2008; Rilling & Van Den Heuvel, 2018; Rolls, 2019; Van Essen et al., 2018; Wu et al., 2016). Given the enormous amount of processing units and information exchange that takes place in the brain, even tiny changes in this sense can significantly improve or hinder computational speed (Hofman, 2012). Another network parameter that is key for connectivity and neural signalling speed is closeness. In this case, the cerebral components closest to all others are the parahippocampal and orbital gyri, and the anterior lobe of the cerebellum.

Additionally, the craniocerebral anatomical network model exhibits the simultaneous presence of two phenotypic patterns, two complementary community structures: a vertical and a longitudinal modular partition (Schuurman & Bruner, 2024). The vertical separation of the craniocerebral network follows the skull's overall morphogenetic organisation. The inferior parts of the primate skull, the viscerocranium and basicranium, are complex anatomical regions with fundamental roles in somatic functionality, including breathing, feeding and posture (Lieberman et al., 2000a). Primary determinants of cerebral spatial arrangement associated with the basicranium include humans' extraordinary base angulation and decreased mandibular ramus breadth (Bastir et al., 2004; Bastir & Rosas, 2005; Lieberman et al., 2000a; McCarthy, 2001). In these regions the skull is expected to exert major spatial constrains on the brain's morphological organisation, particularly in lower parts of the frontal, temporal and limbic lobes, basal and subcortical regions, and the cerebellum (Bastir et al., 2006, 2010; Bruner, 2015; Enlow et al., 1971; Enlow & McNamara, 1973; Lieberman et al., 2000a, 2000b). That is to say, any morphological change observed in inferior cerebral components (e.g. the parahippocampal gyrus) is unlikely to be due to functional adaptation, which is partly a consequence of their physical interaction with elements of the basicranium (e.g. the sphenoid body and lesser wings, or the ethmoid bone). Contrarily, the superior region of the primate skull, the calvaria, is a relatively simpler morphogenetic system, free of interactions with vital organs such as the pharynx (Sperber & Sperber, 2018). Therefore, according to the cranial functional matrix hypothesis, here the skull (e.g. parietal bone) is expected to be moulded by the brain (Moss & Young, 1960; Richtsmeier & Flaherty, 2013). This phenomenon generates a reliable correspondence between cranial and cerebral form (Bruner, 2015; Bruner et al., 2019). Especially noteworthy are the findings of a correlation of shape, but not of size, in the human parietal and occipital bones, meaning when one swells the other becomes flattened and vice versa (Allen et al., 2002; Gunz & Harvati, 2007).

The longitudinal separation of the craniocerebral network probably has to do with the specific morphogenetic arrangement of the three cranial fossae: depressions in the floor of the basicranium, which house the lower parts of the frontal and temporal lobes and the cerebellum. The mixed embryological origins, complex geometry, and multifactorial variability of the basicranium entail distinct local structural influences on each cranial fossa, causing only a modest level of reciprocal morphological integration among them (Bruner & Ripani, 2008; Jeffery & Spoor, 2004; Lieberman et al., 2000a). Presently, this spatial arrangement is paralleled in the brain by a division of its anterior and posterior elements by the midbrain region. In previous work, the longitudinal division of the brain has also been observed to be mediated by the pericentral and cingulate gyri (Bruner, 2022; Bruner et al., 2019). However, here the former appear to play no major role in the overall architecture, while the latter seems more related with the vertical division of the brain. In the anterior cranial fossa, there is a spatial conflict between the frontal lobes and the upper face (orbits and eyeballs) (Pereira-Pedro et al., 2017). This is especially relevant for modern humans and Neandertals, two species that display the largest overlap between the frontal lobes and the orbital roof (Bruner & Holloway, 2010). Correspondingly, the topology of the frontal lobes seems more constrained by influences of the skull than by other cerebral elements (Bruner et al., 2019): the most relevant physical interactions of its components are, consistently, the frontal, parietal and ethmoid bones, and the sphenoid body and lesser wings. At the middle fossa, there is a further spatial conflict among the temporal lobes, mandible, ethmomaxillary block and orbits (Bastir et al., 2004; Bastir & Rosas, 2005, 2006; Bruner et al., 2017; McCarthy, 2001; Pereira-Pedro et al., 2017; Pereira-Pedro & Bruner, 2022). Our previous network approaches to the modern human brain point consistently at the temporal lobes as

morphologically complex regions, subjected to intrinsic spatial constraints both at their external surface (Bruner et al., 2019) and in their deeper medial limbic counterpart, the parahippocampal gyrus (Schuurman & Bruner, 2023). This craniocerebral spatial conflict in the middle cranial fossa is made clear, for example, by the intricacy of the temporal lobes' sulcal imprints on the endocranial surface (e.g. Rosas et al., 2014).

In relation to the asymmetries found in the different communities, these are interpreted as partial overlap between distinct modules (Schuurman & Bruner, 2024). In the case of the cingulate gyrus, the difference between the left and right side is interpreted as the consequence of its extraordinary bridging role. This means that the cingulate gyrus is partially influenced by several regions of the brain and, thus, by several morphological modules. In other words, different anatomical elements display a distinct level of sensitivity to morphological changes, depending on the number of other elements or modules that can influence or constrain their topological environment. Some elements are influenced only by neighbouring regions, or by regions of the same module, while others are influenced by distinct blocks, generally because of their intermediate position. In the case of the insula and the claustrum, it is possible that their imbalance appears simply by virtue of their relatively low number of interactions, and that their sensitivity is hence due to minor random factors (such as the asymmetry found in the cingulate gyrus) that can determine the linkage to one module or another.

As a final remark, we should remind that the different patterns of modularity presented in distinct analyses should not be intended as contradictory, but complementary. When using models, outputs must be interpreted according to the elements and parameters involved. In the case of anatomical networks, modularity patterns concern the degree of linkage between the specific anatomical parts considered in the model. In this sense, this degree is different when considering different groups of elements (e.g. the cortex, the whole brain, or the craniocerebral complex). The different results should hence be used to converge into a single comprehensive view of the topological organisation.

4.3 | Limitations and future steps

Network theory relies on models that are inevitably built on a set of assumptions and criteria (Butts, 2009). One such criterion is the number of nodes and edges included, which determines the model's complexity, resolution, sensitivity, and stability. We chose to subdivide the adult skull according to its number of bony elements at birth, instead of considering only a selection of endocranial bone elements (Bruner et al., 2019). The number of nodes and edges included influences the results of network analysis, as they represent a mathematical description of the model's properties. Hence, the results of network analysis should always be considered in light of the model in question (Rasskin-Gutman & Esteve-Altava, 2014). Anatomical network analysis should be intended as an exploratory tool to investigate the topological components fundamental to the craniocerebral geometric balance and to identify underlying phenotypic patterns of spatial arrangement. Beyond modelling, specific hypotheses should be tested on experimental grounds, or using developmental series able to reveal the dynamic aspects of the underlying morphogenetic system. Results that warrant empirical testing include the conservation of the parahippocampal gyrus across the tetrapod clade, or the effect of skull form on the brain in lissencephalic versus gyrencephalic specimens. This could be performed in mice by inducing cortical gyrification and syndromic craniosynostosis (Chizhikov et al., 2019; Lee et al., 2019). Notwithstanding, additional network issues should still be considered, to further improve these topological considerations. First, the inclusion of weights to the networks' edges should be evaluated, as to represent the physical extension of the interactions among craniocerebral components. Second, the use of probabilistic atlases instead of a consensus one, thereby including humans' intrinsic craniocerebral variation and improving the model's resolution. Third, future research could expand upon the craniocerebral network model by incorporating additional soft tissues of the braincase (such as the meninges, the vascular system, and the cranial muscles), or by extending the analysis to other species of primates as to define the polarity of the changes that we observe. These improvements to the anatomical network model of the human skull and brain are under development and aim to provide an integral view of the evolution of human head morphology.

ACKNOWLEDGEMENTS

T.S. is funded by Fundación Atapuerca/CaixaBank. E.B. is funded by Project PID2021-122355NB-C33 financed by MCIN/AEI/10.13039/501100011033/ FEDER, UE, and by the Istituto Italiano di Antropologia (ISItA).

CONFLICT OF INTEREST STATEMENT

The authors declare no conflict of interest.

DATA AVAILABILITY STATEMENT

The data that support the findings of this study are available from the corresponding author upon reasonable request.

ORCID

Tim Schuurman https://orcid.org/0000-0002-9780-0973
Emiliano Bruner https://orcid.org/0000-0002-6686-4616

REFERENCES

Allen, J.S., Damasio, H. & Thomas, J.G. (2002) Normal neuroanatomical variation in the human brain: an MRI-volumetric study. *American Journal of Physical Anthropology*, 118, 341–358.

Bastian, M., Heymann, S. & Jacomy, M. (2009) Gephi: an open source software for exploring and manipulating networks. *International AAAI Conference on Weblogs and Social Media*, 3, 361–362.

Bastir, M. (2008) A systems-model for the morphological analysis of integration and modularity in human craniofacial evolution. *Journal of Anthropological Sciences*, 86, 37–58.

Bastir, M. & Rosas, A. (2005) Hierarchical nature of morphological integration and modularity in the human posterior face. *American Journal of Physical Anthropology*, 128, 26–34.

Bastir, M. & Rosas, A. (2006) Correlated variation between the lateral basicranium and the face: a geometric morphometric study in different human groups. *Archives of Oral Biology*, 51, 814–824.

Bastir, M., Rosas, A. & Kuroe, K. (2004) Petrosal orientation and mandibular ramus breadth: evidence for an integrated petroso-mandibular developmental unit. *American Journal of Physical Anthropology*, 123, 340–350.

Bastir, M., Rosas, A., Lieberman, D.E. & O'Higgins, P. (2008) Middle cranial fossa anatomy and the origin of modern humans. *Anatomical Record*, 291, 130–140.

Bastir, M., Rosas, A. & O'Higgins, P. (2006) Craniofacial levels and the morphological maturation of the human skull: spatiotemporal pattern of cranial ontogeny. *Journal of Anatomy*, 209, 637–654.

Bastir, M., Rosas, A., Stringer, C., Manuel Cuétara, J., Kruszynski, R., Weber, G.W. et al. (2010) Effects of brain and facial size on basicranial from in human and primate evolution. *Journal of Human Evolution*, 58, 421–431.

Blondel, V.D., Guillaume, J.L., Lambiotte, R. & Lefebvre, E. (2008) Fast unfolding of communities in large networks. *Journal of Statistical Mechanics: Theory and Experiment*, 10, P10008.

Bruner, E. (2004) Geometric morphometrics and paleoneurology: brain shape evolution in the genus *homo*. *Journal of Human Evolution*, 47, 279–303.

Bruner, E. (2015) Functional craniology and brain evolution. In: Bruner, E. (Ed.) *Human paleoneurology*. Cham: Springer, pp. 57–94.

Bruner, E. (2017) The fossil evidence of human brain evolution. In: Kaas, J. (Ed.) *Evolution of nervous systems*, Vol. 4, 2nd edition. Oxford: Elsevier, pp. 63–92.

Bruner, E. (2019) Human paleoneurology: shaping cortical evolution in fossil hominids. *Journal of Comparative Neurology*, 527, 1753–1765.

Bruner, E. (2022) A network approach to the topological organization of the Brodmann map. *The Anatomical Record*, 305, 3504–3515.

Bruner, E., Amano, H., de la Cuétara, J.M. & Ogihara, N. (2015) The brain and the braincase: a spatial analysis on the midsagittal profile in adult humans. *Journal of Anatomy*, 227, 268–276.

Bruner, E., de la Cuétara, J.M., Masters, M., Amano, H. & Ogihara, N. (2014) Functional craniology and brain evolution: from paleontology to biomedicine. *Frontiers in Neuroanatomy*, 8, 19.

Bruner, E., Esteve-Altava, B. & Rasskin-Gutman, D. (2019) A network approach to brain form, cortical topology and human evolution. *Brain Structure and Function*, 224, 2231–2245.

Bruner, E. & Holloway, R.L. (2010) A bivariate approach to the widening of the frontal lobes in the genus *homo*. *Journal of Human Evolution*, 58, 138–146.

Bruner, E., Pereira-Pedro, A.S. & Bastir, M. (2017) Patterns of morphological integration between parietal and temporal areas in the human skull. *Journal of Morphology*, 278, 1312–1320.

Bruner, E. & Ripani, M. (2008) A quantitative and descriptive approach to morphological variation of the endocranial base in modern humans. *American Journal of Physical Anthropology*, 137, 30–40.

Bullmore, E. & Sporns, O. (2009) Complex brain networks: graph theoretical analysis of structural and functional systems. *Nature Reviews Neuroscience*, 10, 186–198.

Bullmore, E. & Sporns, O. (2012) The economy of brain network organization. *Nature Reviews Neuroscience*, 13, 336–349.

Butts, C.T. (2009) Revisiting the foundations of network analysis. *Science*, 325, 414–416.

Cheverud, J.M. (1996) Developmental integration and the evolution of pleiotropy. *American Zoologist*, 36, 44–50.

Chizhikov, V.V., Iskusnykh, I.Y., Steshina, E.Y., Fattakhov, N., Lindgren, A.G., Shetty, A.S. et al. (2019) Early dorsomedial tissue interactions regulate gyrification of distal neocortex. *Nature Communications*, 10, 5192.

Csardi, G. & Nepusz, T. (2006) The igraph software package for complex network research. *International Journal of Complex Systems*, 1695, 1–9.

Dos Santos, D.A., Fratani, J., Ponssa, M.L. & Abdala, V. (2017) Network architecture associated with the highly specialized hind limb of frogs. *PLoS One*, 12, e0177819.

Dumoncel, J., Subsol, G., Durrleman, S., Bertrand, A., de Jager, E., Oettlé, A.C. et al. (2021) Are endocasts reliable proxies for brains? A 3D quantitative comparison of the extant human brain and endocast. *Journal of Anatomy*, 238, 480–488.

Enlow, D.H., Kuroda, T. & Lewis, A.B. (1971) The morphological and morphogenetic basis for craniofacial form and pattern. *The Angle Orthodontist*, 41, 161–188.

Enlow, D.H. & McNamara, J.A. (1973) The neurocranial basis for facial form and pattern. *The Angle Orthodontist*, 43, 256–270.

Erdös, P. & Rényi, A. (1960) On the evolution of random graphs. *Publications of the Mathematical Institute of the Hungarian Academy of Sciences*, 5, 17–61.

Esteve-Altava, B., Marugán-Lobón, J., Botella, H., Bastir, M. & Rasskin-Gutman, D. (2013) Grist for Riedl's mill: a network model perspective on the integration and modularity of the human skull. *Journal of Experimental Zoology*, 320, 489–500.

Esteve-Altava, B., Marugán-Lobón, J., Botella, H. & Rasskin-Gutman, D. (2011) Network models in anatomical systems. *The Journal of Anthropological Sciences*, 89, 175–184.

Esteve-Altava, B., Marugán-Lobón, J., Botella, H. & Rasskin-Gutman, D. (2013) Structural constraints in the evolution of the tetrapod skull complexity: Williston's law revisited using network models. *Evolutionary Biology*, 40, 209–219.

Esteve-Altava, B., Vallès-Català, T., Guimerà, R., Sales-Pardo, M. & Rasskin-Gutman, D. (2017) Bone fusion in normal and pathological development is constrained by the network architecture of the human skull. *Scientific Reports*, 7, 3336.

Gunz, P. & Harvati, K. (2007) The neanderthal "chignon": variation, integration, and homology. *Journal of Human Evolution*, 52, 262–274.

Hagmann, P., Cammoun, L., Gigandet, X., Meuli, R., Honey, C.J., Wedeen, V.J. et al. (2008) Mapping the structural core of human cerebral cortex. *PLoS Biology*, 6, e159.

Hammer, Ø., Ryan, P. & Harper, D. (2001) PAST: paleontological statistics software package for education and data analysis. *Palaeontologia Electronica*, 4, 9.

Hofman, M.A. (1989) On the evolution and geometry of the brain in mammals. *Progress in Neurobiology*, 32, 137–158.

Hofman, M.A. (2012) Design principles of the human brain: an evolutionary perspective. *Progress in Brain Research*, 195, 373–390.

Hofman, M.A. (2014) Evolution of the human brain: when bigger is better. *Frontiers in Neuroanatomy*, 8, 15.

Holloway, R.L., Broadfield, D.C. & Yuan, M.S. (2004) *Brain endocasts: the paleoneurological evidence*. Hoboken, NJ: Wiley.

Humphries, M.D. & Gurney, K. (2008) Network 'small-world-ness': a quantitative method for determining canonical network equivalence. *PLoS One*, 3, e0002051.

Jeffery, N. (1999) *Fetal development and evolution of the human cranial base*. Doctoral dissertation, University College London. UCL Discovery. Available from: https://discovery.ucl.ac.uk/id/eprint/10101315/

Jeffery, N. & Manson, A. (2023) Postnatal growth and spatial conformity of the cranium, brain, eyeballs and masseter muscles in the macaque (*Macaca mulatta*). *Journal of Anatomy*, 243, 590–604.

Jeffery, N. & Spoor, F. (2004) Ossification and midline shape changes of the human fetal cranial base. *American Journal of Physical Anthropology*, 123, 78–90.

Jeffery, N.S., Sarver, D.C. & Mendias, C.L. (2021) Ontogenetic and in silico models of spatial packing in the hypermuscular mouse skull. *Journal of Anatomy*, 238, 1284–1295.

Kerkman, J.N., Daffertshofer, A., Gollo, L.L., Breakspear, M. & Boonstra, T.W. (2018) Network structure of the human musculoskeletal system shapes neural interactions on multiple time scales. *Science Advances*, 4, eaat0497.

Lee, K.K.L., Stanier, P. & Pauws, E. (2019) Mouse models of syndromic craniosynostosis. *Molecular Syndromology*, 10, 58–73.

Leigh, S.R. (2004) Brain growth, life history, and cognition in primate and human evolution. *American Journal of Primatology*, 62, 139–164.

Lieberman, D.E. (1998) Sphenoid shortening and the evolution of modern human cranial shape. *Nature*, 393, 158–162.
Lieberman, D.E. (2011) *The evolution of the human head*. Cambridge, MA: Harvard University Press.
Lieberman, D.E. & McCarthy, R.C. (1999) The ontogeny of cranial base angulation in humans and chimpanzees and its implications for reconstructing pharyngeal dimensions. *Journal of Human Evolution*, 36, 487–517.
Lieberman, D.E., Ross, C.F. & Ravosa, M.J. (2000a) The primate cranial base: ontogeny, function, and integration. *The Yearbook of Physical Anthropology*, 43, 117–169.
Lieberman, D.E., Ross, C.F. & Ravosa, M.J. (2000b) Basicranial influence on overall cranial shape. *Journal of Human Evolution*, 38, 291–315.
McCarthy, R.C. (2001) Anthropoid cranial base architecture and scaling relationships. *Journal of Human Evolution*, 40, 41–66.
Moss, M.L. & Young, R.W. (1960) A functional approach to craniology. *American Journal of Physical Anthropology*, 18, 281–292.
Murphy, A.C., Muldoon, S.F., Baker, D., Lastowka, A., Bennett, B., Yang, M. et al. (2018) Structure, function, and control of the human musculoskeletal network. *PLoS Biology*, 16, e2002811.
Neubauer, S., Gunz, P. & Hublin, J.J. (2009) The pattern of endocranial ontogenetic shape changes in humans. *Journal of Anatomy*, 215, 240–255.
Neubauer, S. & Hublin, J.J. (2012) The evolution of human brain development. *Evolutionary Biology*, 39, 568–586.
Newman, M.E.J. (2018) *Networks*. Oxford: Oxford University Press.
Newman, M.E.J. & Girvan, M. (2004) Finding and evaluating community structure in networks. *Physical Review E*, 69, 026113.
Pearson, A., Bruner, E. & Polly, P.D. (2023) Updated imaging and phylogenetic comparative methods reassess relative temporal lobe size in anthropoids and modern humans. *American Journal of Biological Anthropoloy*, 180, 768–776.
Pereira-Pedro, A.S. & Bruner, E. (2022) Craniofacial orientation and parietal bone morphology in adult modern humans. *Journal of Anatomy*, 240, 330–338.
Pereira-Pedro, A.S., Masters, M. & Bruner, E. (2017) Shape analysis of spatial relationships between orbito-ocular and endocranial structures in modern humans and fossil hominids. *Journal of Anatomy*, 231, 947–960.
R Core Team. (2023) *R: a language and environment for statistical computing*. Vienna: R Foundation for Statistical Computing. Available from: https://www.R-project.org/
Rashevski, N. (1954) Topology and life: in search of general mathematical principles in biology and sociology. *The Bulletin of Mathematical Biophysics*, 16, 317–348.
Rasskin-Gutman, D. & Buscalioni, A. (2001) Theoretical morphology of the archosaur (Reptilia: Diapsida) pelvic girdle. *Paleobiology*, 27, 59–78.
Rasskin-Gutman, D. & Esteve-Altava, B. (2014) Connecting the dots: anatomical network analysis in morphological EvoDevo. *Biological Theory*, 9, 178–193.
Rasskin-Gutman, D. & Esteve-Altava, B. (2018) Concept of burden in evo-devo. In: Nuño de la Rosa, L. & Müller, G.B. (Eds.) *Evolutionary developmental biology*. Cham: Springer.
Richtsmeier, J.T., Aldridge, K., DeLeon, V.B., Panchal, J., Kane, A.A., Marsh, J.L. et al. (2006) Phenotypic integration of neurocranium and brain. *Journal of Experimental Zoology Part B: Molecular and Developmental Evolution*, 306B, 360–378.
Richtsmeier, J.T. & Flaherty, K. (2013) Hand in glove: brain and skull in development and dysmorphogenesis. *Acta Neuropathologica*, 125, 469–489.
Riedl, R. (1978) *Order in living organisms: a systems analysis of evolution*. New York, NY: Wiley.
Rilling, J.K. (2023) Human temporal lobes have been reorganized: a response to Pearson et al, "updated imaging and phylogenetic comparative methods reassess relative temporal lobe size in anthropoids and modern humans". *American Journal of Biological Anthropology*, 182, 3–6.
Rilling, J.K. & Seligman, R.A. (2002) A quantitative morphometric comparative analysis of the primate temporal lobe. *Journal of Human Evolution*, 42, 505–533.
Rilling, J.K. & Van Den Heuvel, M.P. (2018) Comparative primate connectomics. *Brain, Behavior and Evolution*, 91, 170–179.
Rolls, E.T. (2019) The cingulate cortex and limbic systems for emotion, action, and memory. *Brain Structure and Function*, 224, 3001–3018.
Ronan, L. & Fletcher, P.C. (2015) From genes to folds: a review of cortical gyrification theory. *Brain Structure and Function*, 220, 2475–2483.
Rosas, A., Peña-Melián, A., García-Tabernero, A., Bastir, M. & De La Rasilla, M. (2014) Temporal lobe sulcal pattern and the bony impressions in the middle cranial fossa: the case of the El Sidrón (Spain) Neandertal sample. *The Anatomical Record*, 297, 2331–2341.
Ross, C.F. & Ravosa, M.J. (1993) Basicranial flexion, relative brain size, and facial kyphosis in nonhuman primates. *American Journal of Physical Anthropology*, 91, 305–324.
Schuurman, T. & Bruner, E. (2023) A comprehensive anatomical network analysis of human brain topology. *Journal of Anatomy*, 242, 973–985.
Schuurman, T. & Bruner, E. (2024) Modularity and community detection in human brain morphology. *The Anatomical Record*, 307, 345–355.
Sperber, G.H. & Sperber, S.M. (2018) *Craniofacial embyrogenetics and development*, 3rd edition. Raleigh, NC: PMPH-USA.
Spoor, F., O'Higgins, P., Dean, C. & Lieberman, D.E. (1999) Anterior sphenoid in modern humans. *Nature*, 397, 572.
Toro-Ibacache, V., Muñoz, V.Z. & O'Higgins, P. (2016) The relationship between skull morphology, masticatory muscle force and cranial skeletal deformation during biting. *Annals of Anatomy-Anatomischer Anzeiger*, 203, 59–68.
Van Essen, D.C., Donahue, C.J. & Glasser, M.F. (2018) Development and evolution of cerebral and cerebellar cortex. *Brain, Behavior and Evolution*, 91, 158–169.
White, T.D., Black, M.T. & Folkens, P.A. (2013) Chapter 3 – Skull: cranium and mandible. In: *Human osteology*, 3rd edition. Cambridge, MA: Academic Press, pp. 43–100.
Wilder, L. & Semendeferi, K. (2022) Infant brain development and plasticity from an evolutionary perspective. In: Hart, S.L. & Bjorklund, D.F. (Eds.) *Evolutionary perspectives on infancy*. Cham: Springer, pp. 39–58.
Wu, Y., Sun, D., Wang, Y., Wang, Y. & Ou, S. (2016) Segmentation of the cingulum bundle in the human brain: a new perspective based on DSI tactography and fiber dissection study. *Frontiers in Neuroanatomy*, 10, 84.
Wuchty, S., Ravasz, E. & Barabási, A.-L. (2006) The architecture of biological networks. In: Deisboeck, T.S. & Kresh, J.Y. (Eds.) *Complex systems science in biomedicine*, 1st edition. Boston, MA: Springer, pp. 165–181.
Zilles, K., Armstrong, E., Moser, K.H., Schleiler, A. & Stephan, H. (1989) Gyrification in the cerebral cortex of primates. *Brain Behaviour and Evolution*, 34, 143–150.
Zilles, K., Armstrong, E., Schleiler, A. & Kretschman, H.J. (1988) The human pattern of gyrification in the cerebral cortex. *Anatomy and Embryology (Berlin)*, 179, 173–179.
Zilles, K., Palomero-Gallagher, N. & Amunts, K. (2013) Development of cortical folding during evolution and ontogeny. *Trends in Neurosciences*, 36, 275–284.

How to cite this article: Schuurman, T. & Bruner, E. (2024) An inclusive anatomical network analysis of human craniocerebral topology. *Journal of Anatomy*, 245, 686–698. Available from: https://doi.org/10.1111/joa.14068